

Mutual information in time-varying biochemical systems

Filipe Tostevin* and Pieter Rein ten Wolde

FOM Institute AMOLF, Science Park 104, 1098XG Amsterdam, The Netherlands

(Dated: June 16, 2010)

Cells must continuously sense and respond to time-varying environmental stimuli. These signals are transmitted and processed by biochemical signalling networks. However, the biochemical reactions making up these networks are intrinsically noisy, which limits the reliability of intracellular signalling. Here we use information theory to characterise the reliability of transmission of time-varying signals through elementary biochemical reactions in the presence of noise. We calculate the mutual information for both instantaneous measurements and trajectories of biochemical systems for a Gaussian model. Our results indicate that the same network can have radically different characteristics for the transmission of instantaneous signals and trajectories. For trajectories, the ability of a network to respond to changes in the input signal is determined by the timing of reaction events, and is independent of the correlation time of the output of the network. We also study how reliably signals on different time-scales can be transmitted by considering the frequency-dependent coherence and gain-to-noise ratio. We find that a detector that does not consume the ligand molecule upon detection can more reliably transmit slowly varying signals, while an absorbing detector can more reliably transmit rapidly varying signals. Furthermore, we find that while one reaction may more reliably transmit information than another when considered in isolation, when placed within a signalling cascade the relative performance of the two reactions can be reversed. This means that optimising signal transmission at a single level of a signalling cascade can reduce signalling performance for the cascade as a whole.

I. INTRODUCTION

Cells are continually exposed to a wide range of environmental signals to which they must react. These stimuli are transmitted and processed within the cell by networks of proteins and interactions. However, the biochemical reactions which make up these networks are inherently stochastic events. Recent experiments have shown that fluctuations associated with this spontaneous reaction noise can have significant effects on cell phenotype [1–3]. In signalling networks, the effect of this inevitable biochemical noise will be to disrupt the transmission of signals. Random fluctuations mean that a single input signal can give rise to a distribution of possible responses. Conversely, a particular response can be generated from a number of input signals. This uncertainty compromises the ability of a cell to respond correctly to its environment. It is therefore important to understand how reliably signals can be transmitted through signalling networks in the presence of noise.

A quantitative framework for analysing the reliability of signal communication in the presence of noise is provided by information theory [4]. The application of information theory to neural and sensory signalling has a long history [5–7], with particular focus on the reliable encoding of external stimuli in neuronal spiking patterns (for example [8, 9]). However, the use of these techniques in the analysis of intracellular biochemical signalling and gene-regulatory networks has, until recently, received less attention. In this context a number of studies have con-

sidered the reliability of transmission of signals through specific reaction systems in the presence of noise [10–14] and subject to constraints such as metabolic cost [15, 16]. Additionally the impact of network topology on the transmission of constant signals in generic small gene regulation and protein signalling motifs has been investigated [14, 17–20].

Here we analyse the signalling characteristics of a number of elementary biochemical reactions for time-varying signals. Specifically, the fidelity of information transmission between the input and output signals of a biochemical network is measured by the mutual information. Most previous analyses of the mutual information for simple reaction motifs [12–14, 17–20] have considered only the response of a network to signals which do not change on the time-scale of the network response. For many systems the assumption that the signal is constant may not be valid. Cells are often exposed to rapidly varying environments, to which they should also present a time-varying response. Notably, Levine et al [11] calculated the mutual information of an enzymatic push-pull network in response to an signal pulse. However, they considered only the information about a restricted two-state input signal that can be extracted from the instantaneous output level, and did not take into account the transmission of other dynamical properties of the input. Biochemical networks often respond not only to the instantaneous values of time-varying signals but also to other characteristics of the stimulus. For example, the chemotaxis network of the bacterium *E. coli* is sensitive to changes in the level of chemoattractants in the environment, but adapts to constant signals [21, 22]. Another example of sensitivity to environmental changes is the osmotic shock response in budding yeast, where the cell reacts only to changes in osmotic pressure [23]. Cells can also make

*Electronic address: f.tostevin@amolf.nl

use of temporal properties of signals to encode information. For example, in calcium signalling it is believed that information is encoded in the frequency and duration of Ca^{2+} bursts, rather than the concentration at any point in time [24]. In rat PC-12 cells, stimulation with epidermal growth factor leads to a transient response of the MAP-kinase pathway, while neuronal growth factor leads to a sustained response [25]. In order to understand the function of these signalling systems we must consider the transmission of signals which are a function of time, trajectories, through the network.

We have previously discussed the mutual information rate between trajectories of biochemical networks [26], and applied these techniques to small network motifs. This analysis can readily be extended to networks with an arbitrary number of components and more complex network motifs, such as feedback [27] and feedforward [28] loops. However, in order to make the calculations analytically tractable, even in the simplest cases, we must make a number of simplifying assumptions. In short, we assume that the network of interest can be described by a Gaussian model; that is, the distribution of input or output signal values at any point in time is Gaussian, as is the conditional distribution between any two points. For these approximate model systems the mutual information rate can be calculated analytically. For systems that do not satisfy these assumptions the Gaussian model provides a lower bound on the rate of information transmission.

In this paper we calculate the mutual information between *instantaneous* signals and the information rate for *trajectories* within the Gaussian approximation for a number of elementary biochemical reactions. We discuss in detail the assumptions and validity of this model. Our results show that, for signal trajectories, information is encoded in the timing of reaction events in signalling cascades. We also compare the performance of different reactions in isolation and within a simple linear signalling cascade. We find that while a production reaction can transmit some signals more reliably than an irreversible conversion reaction, when placed within a signalling cascade driven by an external upstream signal the relative performance of the two reactions is reversed. Importantly, this shows that increasing the reliability of signal propagation for a single step in a cascade does not necessarily improve, and can in fact degrade, signalling performance for the cascade as a whole. Our results also show that a detection reaction which irreversibly consumes its signal substrate can allow for more reliable information transmission of an upstream signal by reducing noise propagation through the signalling network.

II. FORMULATION: THE GAUSSIAN MODEL

We aim to quantify the performance of biochemical signalling networks by considering how accurately the network input S can be translated into the network output

X . We additionally allow S and X to vary over time, so the “signal” which the network is required to transmit is the trajectory $S(t)$ over some time interval, and the output is similarly the trajectory $X(t)$. As a measure of signalling performance we use the mutual information [4] between the input and output trajectories. Formally, the mutual information is defined in terms of probability distributions over the possible trajectories,

$$I(S, X) = \int D[S(t)] \int D[X(t)] p(S(t), X(t)) \log \left[\frac{p(S(t), X(t))}{p(S(t))p(X(t))} \right]. \quad (1)$$

However a direct evaluation of Eq. 1, either analytically or numerically, is generally not possible because the space of possible trajectories is infinite-dimensional. In order to proceed we approximate the dynamics of the system by a multivariate Gaussian model, for which the mutual information can be calculated exactly. In this section we discuss the application of the standard Gaussian communication channel model [4] to time-varying biochemical networks, and the assumptions and approximations which go into this model.

We take as the input and output signals the deviations of S and X from their average values, $s(t) = S(t) - \langle S(t) \rangle$ and $x(t) = X(t) - \langle X(t) \rangle$, where $\langle \rangle$ represents averaging over different realisations of the dynamical system. We assume that $s(t)$ and $x(t)$ are jointly-Gaussian processes; that is, the joint probability distribution of any two values of these processes, $p(\alpha(t), \beta(t'))$ for $\alpha, \beta = s$ or x , is a bi-variate Gaussian.

For example, we can construct a vector containing the signal values at discrete sample times, $\mathbf{s} = (s(t_1), s(t_2), \dots, s(t_N))$ and similarly for \mathbf{x} . In general, the trajectories \mathbf{s} and \mathbf{x} can be of different lengths, N_s and N_x . In the Gaussian approximation the joint distribution of (\mathbf{s}, \mathbf{x}) is given by

$$p(\mathbf{s}, \mathbf{x}) = (2\pi)^{-(N_s+N_x)/2} |\mathbf{Z}|^{-1/2} \exp \left[-\frac{1}{2} (\mathbf{s} \ \mathbf{x}) \mathbf{Z}^{-1} \begin{pmatrix} \mathbf{s} \\ \mathbf{x} \end{pmatrix} \right]. \quad (2)$$

The $(N_s + N_x) \times (N_s + N_x)$ covariance matrix \mathbf{Z} has the block form

$$\mathbf{Z} = \begin{pmatrix} \mathbf{C}_{ss} & \mathbf{C}_{xs} \\ \mathbf{C}_{sx} & \mathbf{C}_{xx} \end{pmatrix}, \quad (3)$$

where $\mathbf{C}_{\alpha\beta}$ is an $N_\beta \times N_\alpha$ matrix with elements given by the correlation function $\mathbf{C}_{\alpha\beta}^{ij} = C_{\alpha\beta}(t_j, t_i) = \langle \alpha(t_j) \beta(t_i) \rangle$. Furthermore, the form of Eq. 2 means that the distribution $p(\alpha(t) | \beta(t'))$ of any value conditional on any other is also Gaussian with variance $C_{\alpha\beta}(t, t')$.

Shannon [4] showed that the entropy of an N -variate Gaussian distribution with covariance matrix \mathbf{C} is

$$H_G = \frac{1}{2} \log [(2\pi e)^N |\mathbf{C}|]. \quad (4)$$

From the definition of the mutual information, therefore,

$$I(S, X) = H(S) + H(X) - H(S, X) = \frac{1}{2} \log \left[\frac{|\mathbf{C}_{ss}| |\mathbf{C}_{xx}|}{|\mathbf{Z}|} \right]. \quad (5)$$

The problem of calculating the mutual information between trajectories in the Gaussian model reduces to calculating the determinants of the covariance matrices, a great simplification over the functional integration over ensembles of trajectories in Eq. 1. In this manuscript we shall consider two special cases for which the mutual information can readily be evaluated analytically. Specifically, we shall consider a single instantaneous measurement of the system, corresponding to $N_s = N_x = 1$, and infinite continuous trajectories, $N_s = N_x \rightarrow \infty$ and $t_i - t_{i-1} \rightarrow 0$. In this latter case the mutual information rate can be expressed in terms of the spectra of eigenvalues of the covariance matrices.

One of the crucial assumptions of the Gaussian model is that the input signal is Gaussian distributed. The validity of this assumption for real biological systems is not clear, since typical stimulus distributions have not been measured in most systems. As noted above, we also assume that the marginal or transfer probabilities between any two signal points is Gaussian. In general, this is not exactly true for biochemical systems. For systems that do not have Gaussian statistics, Mitra and Stark [29] showed that an appropriate Gaussian model provides a lower bound on the information rate or channel capacity of the non-Gaussian network. For completeness we reproduce here the arguments of the proof by Mitra and Stark [29]:

1. The channel capacity subject to a power constraint on S is defined as $C(S, X) = \max_{p(s)} I(S, X)$, where the maximisation is over all input distributions satisfying the constraint.
2. We can construct a Gaussian input distribution on S satisfying the power constraint, $p_G(s)$. From the definition of the channel capacity, $C(S, X) \geq I(S_G, X)$, since the Gaussian is not necessarily the optimal input distribution for the channel.
3. We can also construct a multivariate Gaussian model with the same second moments as the non-Gaussian system when the input distribution is chosen to be $p_G(s)$. The mutual information in this case $I(S_G, X_G) \leq I(S_G, X)$. This is essentially because a Gaussian distribution has the largest entropy for a given variance, such that a Gaussian transfer function maximises the uncertainty of the output for a given input.
4. In summary, $I(S_G, X_G) \leq I(S_G, X) \leq C(S, X)$.

For a Gaussian system, the mutual information can be calculated exactly, and the mutual information equals the channel capacity. For systems with a Gaussian input distribution but which are otherwise non-Gaussian, the

mutual information is bounded from below by the mutual information for the Gaussian model *with the same second moments as the non-Gaussian system*. For a general non-Gaussian system with a power constraint, the mutual information calculated in this way is a lower bound on the channel capacity.

Van Kampen's linear noise approximation (LNA) [30] provides a prescription by which we can approximate a network of interest by one which satisfies the requirements of the Gaussian model. In this approximation we assume that the intrinsic noise in the network is Gaussian-distributed and small relative to the mean, and we linearise the network response around steady state. For linear systems it is known that the second moments which are calculated in the LNA are exact [31]. Thus for a linear system the LNA can be used to estimate a lower bound on information transmission, which becomes exact in the limit of small Gaussian noise. However, for non-linear systems we are not guaranteed that the second moments calculated in the LNA are the same as those of the full non-linear system. Therefore, the LNA does not necessarily lead to an appropriate Gaussian model of the network in the sense of providing a bound on the information rate. For some non-linear systems the LNA has also been found to provide an accurate description of the second moments of networks [17, 27, 32, 33], particularly for systems with large molecular copy numbers where non-linear effects are negligible. Crucially, though, it is not necessarily obvious *a priori* for a given non-linear network whether or not the LNA will provide an accurate model. Hence if one wishes to consider non-linear networks in the LNA, it is important to verify that the second moments of the approximate model system match those of the full network, for example with stochastic simulations. In the remainder of this paper we will focus only on linear systems for which the second moments can be calculated exactly.

In the model as described above there is no requirement that the system is in a macroscopic steady state [40]. However, henceforth we shall assume that our systems are in such a steady-state as this simplifies the calculation of the correlation functions. Additionally in steady state the correlation functions depend only on time-differences, $C(t, t') = C(t' - t)$, which restricts the form of the covariance matrices and facilitates calculation of the determinants. Furthermore, the assumption of steady state simplifies the interpretation of the calculated information values.

A. Mutual information between instantaneous measurements

In this section we discuss the mutual information between the instantaneous value of the output signal, $X(t_0)$, and the input signal at the same point in time, $S(t_0)$. The instantaneous mutual information tells us, if we know the output of the network at a particular time,

how much we learn about the current state of the input process. We note that this differs from previous analyses of the mutual information for *constant* signals [12–14, 17–20], because S remains a dynamic variable which changes over time. In particular, we take into account the fact that the correlation timescale of the input signal and the response time of the processing network are both finite. The interplay of changes in the signal and response will be particularly important when these timescales are comparable. The instantaneous mutual information considers not only the “intrinsic” noise in X at constant S due to the stochastic nature of the production and decay reactions, but also the “extrinsic” variability in X which arises from changes in the input signal.

An instantaneous measurement of the input and output signals represents a special case of the Gaussian model in which the input and output vectors are each one-dimensional,

$$p(s, x) = \frac{1}{2\pi|\mathbf{Z}|^{1/2}} \exp\left[-\frac{1}{2}(s \ x) \mathbf{Z}^{-1} \begin{pmatrix} s \\ x \end{pmatrix}\right], \quad (6)$$

and the elements of the matrix \mathbf{Z} are the instantaneous covariances, $\sigma_{\alpha\beta}^2 = \langle \alpha(t_0)\beta(t_0) \rangle$:

$$\mathbf{Z} = \begin{pmatrix} \sigma_{ss}^2 & \sigma_{sx}^2 \\ \sigma_{sx}^2 & \sigma_{xx}^2 \end{pmatrix}. \quad (7)$$

Since we allow both the input and output signals to vary in time, these covariances include the interplay of the input and output signal timescales. From Eq. 6 it follows that the conditional distribution of x given s is

$$p(x|s) = \frac{1}{(2\pi\sigma_{x|s}^2)^{1/2}} \exp\left[-\frac{(x - \langle x|s \rangle)^2}{2\sigma_{x|s}^2}\right], \quad (8)$$

where $\langle x|s \rangle = \sigma_{sx}^2 s / \sigma_{ss}^2$ and $\sigma_{x|s}^2 = |\mathbf{Z}| / \sigma_{ss}^2$. We can therefore define the network gain $g = \sigma_{sx}^2 / \sigma_{ss}^2$ and intrinsic noise $\sigma_{x|s}^2 = \sigma_{xx}^2 - g^2 \sigma_{ss}^2$, and the output signal of the network takes the form $x = gs + \eta_{x|s}$, where $\eta_{x|s}$ is a Gaussian-distributed random variable with variance $\sigma_{x|s}^2$. This is the canonical form of the additive white Gaussian noise channel considered by Shannon and others [4, 34, 35]. We note that in general the gain g defined above differs from the “macroscopic” gain in the steady state values of S and X , $\frac{\partial \langle X \rangle}{\partial \langle S \rangle}$, which characterises the transmission of constant signals.

From the definition of the mutual information,

$$I_{\text{inst}}(S, X) = \frac{1}{2} \log\left(\frac{\sigma_{ss}^2 \sigma_{xx}^2}{|\mathbf{Z}|}\right) = \frac{1}{2} \log\left(1 + \frac{\sigma_{sx}^4}{|\mathbf{Z}|}\right) \quad (9)$$

By comparison of Eq. 9 with the well-known result for the capacity of a Gaussian channel [4], we can interpret this result in terms of signal-to-noise ratio:

$$\frac{\text{Signal}}{\text{Noise}} = \frac{\sigma_{sx}^4}{|\mathbf{Z}|} = \frac{g^2}{\sigma_{x|s}^2} \sigma_{ss}^2. \quad (10)$$

In essence, to reliably detect an input signal s the network gain has to raise the output signal x above the noise level $\sigma_{x|s}^2$. The gain-to-noise ratio $g^2 / \sigma_{x|s}^2$ provides a signal-independent measure of the performance of the network. For a given input signal, we therefore expect that the mutual information is maximised when the ratio $g^2 / \sigma_{x|s}^2$ is maximised. The gain-to-noise ratio is also the Fisher information [35] about the signal s contained in the sample x . For a Gaussian system this is the reciprocal of the average error in estimating s from a given output x .

B. Mutual information rate for infinite trajectories

A second special case of the Gaussian model is the limit of infinite, continuous, trajectories. We define the entropy rate of a Gaussian process as

$$h_G = \lim_{N \rightarrow \infty} \frac{H_G}{N\Delta}, \quad (11)$$

where Δ is the sampling interval of the signal and $T = N\Delta$ is the length of the trajectory. Since we assume that the network is fluctuating around steady state, the covariance between the input (or output) signal at two time points depends only on the time difference between the two samples. The corresponding covariance matrix (\mathbf{C}_{ss} or \mathbf{C}_{xx}) therefore has a Toeplitz structure, which allows us to rewrite the matrix determinant in the limit $N \rightarrow \infty$ in terms of the power spectrum of the signal $P(\omega)$ [34, 35],

$$h_G = \frac{1}{2\Delta} \log(2\pi e) + \frac{1}{4\pi} \int_{-\omega_0}^{\omega_0} d\omega \log P(\omega), \quad (12)$$

where $\omega_0 = \pi/\Delta$ is the angular Nyquist frequency. In effect we have decomposed the signal into an infinite number of independent frequency components with corresponding variance $P(\omega)$. Note that in the limit $\Delta \rightarrow 0$ the entropy rate is not well defined. However, as we will see below, the mutual information rate can remain finite in this limit.

To calculate the mutual information we also need the joint entropy rate $h(S, X)$. The covariance matrix \mathbf{Z} for the combined (\mathbf{s}, \mathbf{x}) signal is not (in general) Toeplitz. However, following [36], the joint entropy rate for a Gaussian system can be written in terms of the (cross-) power spectra of the input and output signals,

$$h(S, X) = \frac{1}{\Delta} \log(2\pi e) + \frac{1}{4\pi} \int_{-\omega_0}^{\omega_0} d\omega \log[P_{ss}(\omega)P_{xx}(\omega) - |P_{sx}(\omega)|^2], \quad (13)$$

where $P_{\alpha\beta}(\omega)$ is the Fourier transform of $C_{\alpha\beta}(t)$. Combining this expression with Eq. 12 and taking the limit $\Delta \rightarrow 0$, the mutual information rate between continuous trajectories can be written as

$$R(S, X) = h(S) + h(X) - h(S, X) \quad (14)$$

$$= -\frac{1}{4\pi} \int_{-\infty}^{\infty} d\omega \log\left[1 - \frac{|P_{sx}(\omega)|^2}{P_{ss}(\omega)P_{xx}(\omega)}\right] \quad (15)$$

We can recognise that the total information rate is the sum of independent Gaussian channels at different frequencies. The output trajectory of the network is, by construction, a stationary Gaussian process. For such a process it is known that the different Fourier components must be statistically independent [34]. In order for this to be realised in a signalling system, we require that an input signal at a specific frequency leads to an output only at a unique frequency; if the network has a response at multiple frequencies, the components of the output at these frequencies will be correlated. This is equivalent to assuming that the network response is linear. Furthermore, the noise in the network must be purely additive. As described above, the LNA provides a prescription for constructing a model system which satisfies these requirements. For systems that are non-linear or non-Gaussian, Eq. 15 provides a bound on the information rate or channel capacity, provided that the power spectra of the full non-linear system are used in the calculation of $R(S, X)$.

How should we interpret the ‘‘rate’’ $R(S, X)$? From Eqs. 11 and 14 we see that $R(S, X) = \lim_{T \rightarrow \infty} I(S, X; T)/T$, the total mutual information for two long trajectories divided by the trajectory length. Thus, $R(S, X)$ is the average mutual information per unit time for a long trajectory. From this definition it also follows that $R(S, X) = \lim_{T \rightarrow \infty} \frac{dI(S, X; T)}{dT}$; $R(S, X)$ is the rate at which we gain information about the input trajectory as the length of both the input and output trajectories is increased. However, some care should be taken with this interpretation. If we record an output trajectory of length T , and then measure for an additional time T' , the total information we have about the input trajectory as a whole will increase by approximately $T'R(S, X)$. However, the additional information we have gained will not be restricted to the new segment of the input signal, but will also be distributed over the original trajectory. Therefore, it is not correct to say that we have learnt $T'R(S, X)$ about the segment $T \leq t \leq T + T'$ of the input trajectory. More generally, there may be additional contributions to the mutual information which are important for short trajectories. When T is comparable to the correlation times of the network we would expect $I(S, X; T)/T$ to deviate from $R(S, X)$.

The ratio $\phi(\omega) = \frac{|P_{sx}(\omega)|^2}{P_{ss}(\omega)P_{xx}(\omega)}$ which appears in Eq. 15 is the *coherence* between $s(t)$ and $x(t)$. This is a standard measure of the correlation between the signals s and x , with $\phi(\omega) = 0$ for independent signals and $\phi(\omega) = 1$ when s completely determines x . We can also define the signal and noise power spectra via analogous expressions to those for instantaneous measurements,

$$\Sigma(\omega) = g^2(\omega)P_{ss}(\omega) = \frac{|P_{sx}(\omega)|^2}{P_{ss}(\omega)} \quad (16)$$

$$N(\omega) = P_{xx}(\omega) - \Sigma(\omega). \quad (17)$$

We can see that the coherence represents the signal fraction of the total output power, $\phi(\omega) = \Sigma(\omega)/[\Sigma(\omega) + N(\omega)]$. The mutual information rate can also be written

in terms of the signal-to-noise ratio,

$$R(S, X) = \frac{1}{4\pi} \int_{-\infty}^{\infty} d\omega \log \left[1 + \frac{\Sigma(\omega)}{N(\omega)} \right], \quad (18)$$

recovering the usual expression for the capacity of a continuous Gaussian channel [34, 35].

From [26] and above we can see that the ability of a network to transmit information in a time-varying signal at a particular frequency is characterised by the frequency-dependent gain-to-noise ratio, $g^2(\omega)/N(\omega)$. To understand signalling performance it is therefore important to consider both the gain and the noise of the network, and not simply the gain or noise in isolation. Furthermore, for systems which satisfy the spectral addition rule [32], meaning that the network dynamics do not affect the input signal itself, the gain-to-noise ratio is signal-independent and characterises the intrinsic transmission characteristics of the network. Knowledge of the gain-to-noise ratio also allows us to calculate the optimal signal that maximises the information rate for a given network, through the ‘‘water-filling’’ approach of Fano [34]. Finally, in the same way as for instantaneous measurements, the gain-to-noise ratio at a specific frequency is the Fisher information provided by the output signal $x(\omega)$ about the input signal $s(\omega)$ at this frequency. Thus, the gain-to-noise ratio is the reciprocal of our uncertainty in estimating the input signal given a particular output.

We saw previously that the entropy rate of a stochastic process in the continuum limit is not well defined, but the mutual information rate can still be calculated. Under what conditions do we find a finite mutual information rate? From Eqs 15 and 18 we can see that the mutual information rate will be divergent if the signal-to-noise ratio $\Sigma(\omega)/N(\omega)$ or coherence $\phi(\omega)$ do not approach zero as $\omega \rightarrow \infty$. The power spectra of biochemical reactions typically take the form of rational polynomials in ω^2 (as we shall see in the following sections). Then the integral in the mutual information rate will converge to a finite value if the signal power decreases more rapidly at high frequencies than the noise power. This characteristic form of the power spectra also often allows us to perform the integral in Eq. 15 or 18 and calculate an explicit expression for $R(S, X)$. To do this we make use of the result that

$$\int_0^{\infty} d\omega \ln \left[\frac{\omega^2 + a^2}{\omega^2 + b^2} \right] = \pi(a - b). \quad (19)$$

Using the properties of the logarithm, this can trivially be extended to an arbitrary number of terms,

$$\int_{-\infty}^{\infty} d\omega \ln \left[\prod_{i=1}^N \frac{\omega^2 + a_i^2}{\omega^2 + b_i^2} \right] = 2\pi \left[\sum_{i=1}^N a_i - \sum_{i=1}^N b_i \right]. \quad (20)$$

We emphasise that for the integral to be cast in this form we require that the coefficient of the leading order term in both the denominator and numerator of Eq. 20 is 1. Then calculating $R(S, X)$ reduces to finding the roots

Motif	Reactions
(I)	$\emptyset \xrightarrow{\kappa} S \quad S \xrightarrow{\lambda} \emptyset$ $S \xrightleftharpoons[\mu]{\rho=kW} X$
(II)	$\emptyset \xrightarrow{\kappa} S \quad S \xrightarrow{\lambda} \emptyset$ $S \xrightarrow{\rho} X \quad X \xrightarrow{\mu} \emptyset$
(III)	$\emptyset \xrightarrow{\kappa} S \quad S \xrightarrow{\lambda} \emptyset$ $S \xrightarrow{\rho} S + X \quad X \xrightarrow{\mu} \emptyset$

TABLE I: Summary of the three elementary reaction motifs. In motif I we assume that the number of W proteins is sufficiently large that the rate ρ can be taken to be constant.

of polynomials which are constructed from the network power spectra.

Can we still compare the performance of networks with a divergent information rate? In these networks the coherence and signal-to-noise ratio approach to some non-zero value as $\omega \rightarrow \pm\infty$. Rather than Eq. 20, the integral in the expression for the mutual information rate will have the form

$$\int_{-\omega_0}^{\omega_0} d\omega \ln \left[k \prod_{i=1}^N \frac{\omega^2 + a_i^2}{\omega^2 + b_i^2} \right] = 2\omega_0 \ln k + 2\omega_0 \ln \left[\prod_{i=1}^N \frac{\omega_0^2 + a_i^2}{\omega_0^2 + b_i^2} \right] + 4 \sum_{i=1}^N \left(a_i \arctan \frac{\omega_0}{a_i} - b_i \arctan \frac{\omega_0}{b_i} \right). \quad (21)$$

In the limit of $\Delta \rightarrow 0$ and hence $\omega_0 = \pi/\Delta \rightarrow \infty$ the last two terms above can be neglected. Information transmission for these networks is therefore dominated by high-frequency components, and can be characterised by the constant k . The values of k for different networks can therefore be used to compare their relative information rates.

III. RESULTS

In this section we present results for some elementary molecular reactions, considered previously [26, 32] and summarised in Table I. These reaction schemes are significant because they exemplify the three basic ways in which S can directly drive the production of X : reversible conversion between S and X ; irreversible conversion from S to X ; and stimulating production of X without consuming an S molecule. Since these schemes feature only first-order reactions the covariances and power spectra can be calculated exactly from the chemical master equation [31].

A. Instantaneous mutual information

1. Motif I: Reversible binding

This motif describes the association and disassociation of a signalling molecule, S , and a receptor, W , to form an active complex, X . We assume that W is present at high copy numbers, such that its depletion due to binding S can be neglected. In this case we consider the “signal” we wish to detect to be the total number of both bound and unbound signalling molecules, $S_T(t_0) = S(t_0) + X(t_0)$. For this motif the covariances are

$$\sigma_{s_T s_T}^2 = \langle S_T \rangle, \quad \sigma_{s_T x}^2 = \sigma_{x x}^2 = \langle X \rangle, \quad (22)$$

which gives for the instantaneous mutual information

$$I_{\text{inst}}(S_T, X) = -\frac{1}{2} \log \left(1 - \frac{\rho}{\rho + \mu} \right) = -\frac{1}{2} \log \left(1 - \frac{\langle X \rangle}{\langle S_T \rangle} \right). \quad (23)$$

The instantaneous mutual information between X and S_T is determined simply by the fraction of S_T which is in the bound (X) state on average. Indeed the average statistics of this binding reaction are simply those of a binomial distribution. Each molecule in the system can be in two states: the bound X state with probability $\rho/(\rho + \mu) = \langle X \rangle/\langle S_T \rangle$, or the unbound S state with probability $\langle S \rangle/\langle S_T \rangle$. Since each molecule is independent, if there are N_{S_T} molecules in the system in total, the expected number of X molecules will be $N_{S_T} \langle X \rangle/\langle S_T \rangle = g N_{S_T}$, and the variance in the number of X molecules will be $N_{S_T} g(1-g)$. Averaging over all possible values of S_T , the intrinsic noise in X is $\sigma_{x|s_T}^2 = \langle S_T \rangle g(1-g)$. For instantaneous signals, the time-scales of the binding and dissociation reactions are not important for information transmission, but only their ratio. This is because we wish to estimate only the current state of the system, and we are not concerned with how rapidly the state of the system changes.

2. Motif II: Irreversible modification

This motif is characterised by the irreversible conversion of an S molecule to an X , $S \rightarrow X$. Such a reaction could represent irreversible post-transcriptional modification of a protein such as cleavage, or binding of a ligand to a receptor followed by rapid endocytosis of the resulting complex. For this motif the covariance $\sigma_{sx}^2 = 0$. The number of X molecules present in the system depends only on how many S molecules have been converted to X in the past. If the production of different S molecules occurs independently, then the instantaneous values of S and X are uncorrelated since the S molecules that have previously decayed are uncorrelated from those that are currently present in the system. Hence the instantaneous mutual information between a single measurement of X and the simultaneous value of S is zero; measuring X

tells us nothing about how many S molecules are currently present in the system.

Note however that if there are correlations between the production of different S molecules, such as if S molecules are produced in bursts, then the instantaneous S and X values become correlated and the instantaneous mutual information will be non-zero. Suppose that S molecules are produced instead via the reaction $\emptyset \xrightarrow{\kappa} nS$. Then the mutual information between instantaneous values of S and X is given by

$$I_{\text{inst}}(S, X) = -\frac{1}{2} \log \left(1 - \frac{(n-1)^2 \rho \mu}{(n+1)(\lambda + \mu + \rho)(2\lambda + 2\mu + (n+1)\rho)} \right). \quad (24)$$

Interestingly, for a fixed production rate of X , ρ , the mutual information can be optimised by choosing

$$\mu_{\text{opt}} = \sqrt{(\lambda + \rho)(\lambda + \frac{n+1}{2}\rho)}, \quad (25)$$

while for a fixed degradation rate of X , μ , information is maximised for

$$\rho_{\text{opt}} = (\lambda + \mu) \sqrt{\frac{2}{n+1}}. \quad (26)$$

These optima are the result of a trade-off between the probability that when we observe an X molecule other S molecules produced in the same burst are still in the system, and the probability of observing an X molecule at all, as depicted in Fig. 1. For example, if the production rate of X is too large, all S molecules rapidly decay to X . Since the probability of S molecules from the same burst remaining in the system is low, we lose the ability to predict the value of S . If ρ is too small, the chance of a single X molecule being produced in a burst becomes small and we again lose information, this time about the bursts which go undetected. Similar arguments apply for μ : if μ is too small then over the lifetime of X the S molecules from the same burst will typically either have been degraded or also have decayed to X ; if we make μ too large then we very rarely find an X in the system, and hence on average we gain little information about S . Note that Eqs 25 and 26 cannot both be satisfied simultaneously - there are no isolated optimal parameter combinations.

3. Motif III: Production

This motif may represent an effective coarse-grained model of an enzymatic reaction or of protein production in which fast reaction steps have been integrated out. For this motif the covariances are:

$$\sigma_{ss}^2 = \langle S \rangle, \quad \sigma_{sx}^2 = \frac{\rho \langle S \rangle}{\lambda + \mu}, \quad \sigma_{xx}^2 = \langle X \rangle \left(1 + \frac{\rho}{\lambda + \mu} \right). \quad (27)$$

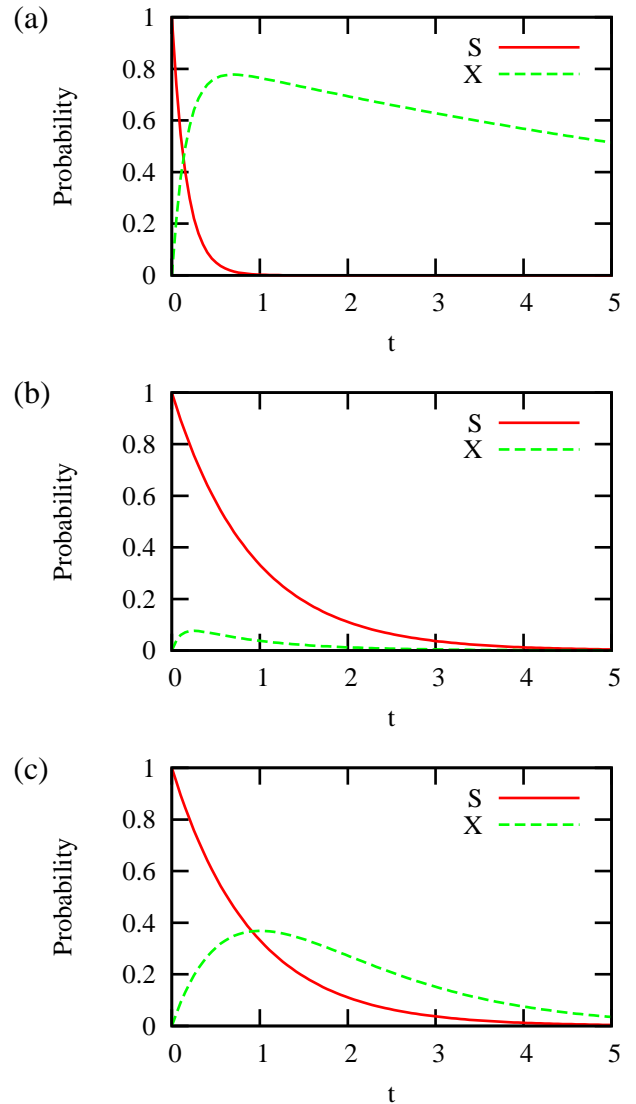


FIG. 1: Probability of a molecule produced at $t = 0$ being in each molecular state of motif II as a function of time for different reaction rates. (a) When $\rho \gg \mu, \lambda$, S molecules rapidly decay to X , but for most of the lifetime of X the chance of an S molecule from the same burst being present is small. Parameters: $\mu = 0.1$, $\lambda = 1$, $\rho = 5$. (b) When $\mu \gg \rho, \lambda$, S molecules which decay to X are rapidly degraded. Therefore the probability of observing an X molecule is small, and little information can be gained. Parameters: $\mu = 10$, $\lambda = 0.1$, $\rho = 1$. (c) Information is maximised when there is a significant probability of finding both S and X molecules. The figure shows an optimal choice of ρ for burst size $n = 2$, $\mu = 0.9$, $\lambda = 0.1$: $\rho = 1$.

The gain is given by $g = \rho/(\lambda + \mu)$, and describes the average response of the output signal X to a perturbation in the input signal. Suppose we initially have no S or X molecules present in the system. We then introduce a single S molecule at $t = 0$. The survival probability for this S molecule, the probability

that it has not yet decayed at time t , will be exponentially distributed with a mean lifetime of $1/\lambda$. If the S molecule has not decayed at t , the mean number of X molecules present will be $\bar{X}(t) = \rho[1 - \exp(-\mu t)]/\mu$. Now we observe the system at a time $t > 0$ chosen according to the probability that the S molecule is still present. This time will then be drawn from the distribution $p(t) = \exp(-\lambda t) / [\int_0^\infty \exp(-\lambda t) dt] = \lambda \exp(-\lambda t)$, and the mean number of X molecules that we will observe is $\int_0^\infty p(t) \bar{X}(t) dt = \rho/(\lambda + \mu)$. We can therefore see that the gain directly measures the typical change we observe in the number of X molecules if the input signal changes by one S molecule.

The instantaneous mutual information is given by

$$I_{\text{inst}}(S, X) = -\frac{1}{2} \log \left[1 - \frac{\rho\mu}{(\lambda + \mu)(\lambda + \mu + \rho)} \right]. \quad (28)$$

We see that $I_{\text{inst}}(S, X)$ has a maximum as a function of μ at

$$\mu_{\text{opt}} = \lambda \sqrt{1 + \frac{\rho}{\lambda}}. \quad (29)$$

This optimal value appears as a result of the interplay between intrinsic noise and temporal correlations in the system. When $\mu \gg \lambda$, intrinsic fluctuations in X are much more rapid than the systematic changes in X due to variations in S . In this case, the instantaneous statistics of X are approximately those of a simple Poisson birth-death process in response to a constant S input. The gain is $g = \rho/(\mu + \lambda) \approx \rho/\mu = \langle X \rangle / \langle S \rangle$, the number of X molecules per S which would be observed for a constant S signal. The noise variance in X is approximately that of a Poisson process, $\sigma_{x|s}^2 \approx \langle X \rangle \sim \mu^{-1}$. While increasing μ decreases the absolute noise strength, the relative noise in the mean $\sigma_{x|s}^2 / \langle X \rangle^2$ increases. Since signalling fidelity depends on the ratio $g^2 / \sigma_{x|s}^2 \propto \langle X \rangle^2 / \sigma_{x|s}^2$, increasing μ decreases the gain-to-noise ratio and reduces the transmitted information. In the opposite limit, when $\mu \ll \lambda$, the output signal X effectively integrates over variations in S . In this case the gain is $g = \rho/(\mu + \lambda) \approx \rho/\lambda$, the mean number of X molecules produced during the lifetime of an S molecule. Since the typical lifetime of X is long compared to that of S we can assume that no X molecule decays before the S from which it was produced. Once we are in this regime further decreasing μ has no effect on our ability to amplify the incoming signal, which is instead limited by the lifetime of S ; integrating for a longer time provides no further benefit. The intrinsic noise variance, however, is still proportional to $\langle X \rangle$ and hence increases as μ is decreased. As a result, for small μ the gain-to-noise ratio goes as $g^2 / \sigma_{x|s}^2 \sim \mu$. The precise value of the optimal decay rate also depends on the production rate of X , ρ , since this determines the time-scale of fluctuations in S to which X can respond.

B. Mutual information rate

For the reactions shown in Table I the power spectra can readily be calculated [31, 32]. Some results for these motifs were presented in [26]. Here we extend the discussion of these results.

1. Motif I

For reaction motif I we again consider the input signal to be $s_T(t) = s(t) + x(t)$. For this motif, the gain-to-noise ratio between the signals $s_T(t)$ and $x(t)$ is given by

$$\frac{g^2(\omega)}{N(\omega)} = \frac{\rho}{2\kappa} \frac{\lambda(\mu + \lambda + \rho)^2}{[\omega^2 + (\mu + \rho)^2 + \rho\lambda]}. \quad (30)$$

We see that information capacity of the network decreases at high frequencies. This network motif effectively acts as a low-pass filter for information. The binding and unbinding reactions cannot track extremely rapid changes in S or X , and therefore high-frequency components of the $s_T(t)$ signal are not transmitted to $x(t)$.

The mutual information rate for this motif can be calculated by performing the integral in Eq. 15, and is given (in nats per unit time) by

$$R(S_T, X) = \frac{\lambda}{2} \left[\sqrt{1 + \beta} + \sqrt{\beta + [\beta + \alpha]^2} - (1 + \alpha + \beta) \right], \quad (31)$$

where $\alpha = \mu/\lambda$ and $\beta = \rho/\lambda$ are respectively the rates of the dissociation and association reactions relative to the lifetime of S . The mutual information rate increases with increasing β and decreases with increasing α . Therefore, as for instantaneous measurements, the amount of information about $s_T(t)$ which we can extract from the trace $x(t)$ increases as the average fraction of molecules in the X state, which is determined by $\rho/\mu = \beta/\alpha$, increases. However, unlike the instantaneous mutual information, the information rate between trajectories does depend on the absolute binding and unbinding rates and not just their ratio. This is because the mutual information rate takes into account the timescale on which the number of X molecules is able to track changes in the number of S molecules. It should also be noted that changing ρ or μ also affect the statistics of the input signal $s_T(t)$, since molecules are protected from degradation while in the X state. This means that the entropy of the input distribution will change as ρ or μ are varied.

2. Motif II

The coherence for this motif is $\phi(\omega) = \rho/4(\rho + \lambda)$, independent of ω . The integral in Eq. 15 is therefore divergent, giving an infinite information rate. In reality, the integral of the mutual information rate should be truncated at some large but finite frequency, since the

biochemical reactions which we have modelled as instantaneous jump processes actually take some finite time to occur. Nevertheless, we can conclude that observing the trajectory $x(t)$ provides a large amount of information about the trajectory $s(t)$ because for every production event of X we know when one S molecule has decayed. However, we do not have a complete knowledge of the input signal $s(t)$ and thus the coherence remains less than 1. We can see that for $\lambda \gg \rho$, $\phi \rightarrow 0$. Since the majority of S molecules are degraded directly, and do not decay via the X form, most of the molecules which pass through the system are never observed in the output signal. Hence the fraction of the input signal which we measure will be very small. Conversely, when $\rho \gg \lambda$, $\phi \approx 1/4$. In this case we observe the decay of all S molecules, but we still have some uncertainty about their production times.

We note also that signalling fidelity, as determined by either the coherence or signal-to-noise ratio, is independent of the decay rate of X , μ . Since decay events of X occur independently of the number of S molecules present, they contribute no information about the input signal. We can understand this by considering the timing of production and decay events in the trajectory of X . Indeed, the trajectory of the number of X molecules as a function of time will consist of discrete steps at which X molecules are produced and decay. Apart from a constant offset which can be absorbed into $\langle X \rangle$, the trajectory $x(t)$ is completely described by the sequence of times at which the number of X molecules increase and decrease, $\{t_+\}$ and $\{t_-\}$ respectively. We can therefore write the probability of a particular trajectory as $p(x(t)) = p(\{t_+\}, \{t_-\}) = p(\{t_+\})p(\{t_-\}|\{t_+\})$. The production of X molecules is regulated by the signal S , but their decay is not. That is, the timing of production events is dependent on the input $s(t)$, but the timing of decay events is determined solely by the intrinsic dynamics of X and therefore does not depend on S explicitly. In this case, we can also factorise the conditional probability of a given trajectory $p(x(t)|s(t)) = p(\{t_+\}|s(t))p(\{t_-\}|\{t_+\})$. The mutual information can then be written as

$$I(s(t), x(t)) = \int D[s(t)] \int D\{t_+\} \int D\{t_-\} p(s(t), \{t_+\}, \{t_-\}) \log \left[\frac{p(s(t))p(\{t_+\}|s(t))p(\{t_-\}|\{t_+\})}{p(s(t))p(\{t_+\})p(\{t_-\}|\{t_+\})} \right], \quad (32)$$

where $D\{t\}$ represent integration over all possible sequences of event times. The argument of the logarithm is independent of $\{t_-\}$, and hence this integral can be performed trivially. We are left with exactly the mutual information between $s(t)$ and $\{t_+\}$,

$$I(s(t), x(t)) = I(s(t), \{t_+\}). \quad (33)$$

This result shows that the information about S which can be extracted from $x(t)$ is contained specifically in the timing of X production events.

The discussion above assumes that individual production and decay steps can be resolved and that the timing of all events is known exactly, and thus is only valid if we can observe the continuous trajectory $x(t)$ on all timescales. If on the other hand we only have a discrete sampling $\mathbf{x} = (x(t_1), x(t_2), \dots, x(t_N))$, then the degradation reactions of X increase our uncertainty about S . If we observe that the number of X molecules has changed by $n = x(t_i) - x(t_{i-1})$ over the interval $[t_{i-1}, t_i]$, then we can conclude that the number of production events in the corresponding interval minus the number of degradation events must equal n . However, we do not know exactly how many production and decay events have taken place, and therefore the accuracy with which we can estimate the input trajectory $s(t)$ is reduced.

3. Motif III

For this motif the gain-to-noise ratio is

$$\frac{g^2(\omega)}{N(\omega)} = \frac{\rho}{2\langle S \rangle}, \quad (34)$$

independent of ω . This motif is therefore able to transmit signals at all frequencies equally well. However, we note that both the gain and noise,

$$g^2(\omega) = \frac{\rho^2}{\omega^2 + \mu^2} \quad (35)$$

$$N(\omega) = \frac{2\rho\langle S \rangle}{\omega^2 + \mu^2} \quad (36)$$

decrease at frequencies larger than μ . Both the input signal and the intrinsic noise in X are effectively integrated over the lifetime of X molecules, $1/\mu$, and so are attenuated at high frequencies. It should be noted that while information can be reliably encoded at high frequencies in the signal $x(t)$, the power associated with these variations, $g^2(\omega)P_{ss}(\omega)$, may be small. Therefore, if this signal is taken as the input to another downstream process, these signals may be difficult to decode. For example, intrinsic noise in the detection of X by the downstream network may overwhelm the small amplitude signal at high frequencies [26].

The coherence for this motif is

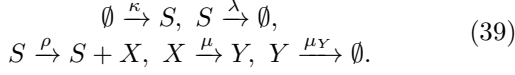
$$\phi(\omega) = \frac{\rho\lambda}{\omega^2 + \lambda(\lambda + \rho)}, \quad (37)$$

showing that the information content of the output signal decreases at high frequencies. This is because the coherence depends on the input power spectrum $P_{ss}(\omega)$, which itself scales as ω^{-2} for $\omega \gg \lambda$; the information content of the input signal is itself reduced at high frequencies. The mutual information rate (in nats per unit time) for this motif is

$$R(S, X) = \frac{\lambda}{2} \left[\sqrt{1 + \rho/\lambda} - 1 \right]. \quad (38)$$

As we saw for motif II, both the coherence and information rate are independent of μ , the decay rate of X . As discussed above, since decay events of X occur independently of the input signal S , the information we can gain about the input signal is the information encoded in the production of X .

We may therefore be tempted to conclude that the decay events of X contain no information about the input signal $s(t)$. This is not entirely true. The information encoded in the decay events of X can be quantified by considering a modified network combining motifs II and III as follows:



As we saw in the previous section, in motif II information about the input signal is encoded in the timing of X production reactions. Similarly, in the set of reactions in Eq. 39 information about S will be encoded in the timing of Y production reactions. Since the reactions producing Y correspond to decays of X , the mutual information between $s(t)$ and $y(t)$ will also be the mutual information between $s(t)$ and the decays of X . In the limit $\mu \rightarrow \infty$, this set of reactions reduces to motif III: as X molecules decay immediately the two reactions $S \xrightarrow{\rho} S + X$ and $X \xrightarrow{\mu} Y$ are effectively combined into $S \xrightarrow{\rho} S + Y$. However, for finite μ we find that the mutual information rate between S and Y ,

$$R(S, Y) = \frac{\lambda}{2} \left[\sqrt{1 + 2\alpha\sqrt{1 + \beta} + \alpha^2} - (1 + \alpha) \right], \quad (40)$$

where $\alpha = \mu/\lambda$ and $\beta = \rho/\lambda$, is reduced compared to Eq. 38. Additionally, the gain-to-noise ratio and coherence,

$$\frac{g^2(\omega)}{N(\omega)} = \frac{\rho}{2\langle S \rangle} \frac{\mu^2}{\omega^2 + \mu^2}, \quad (41)$$

$$\phi(\omega) = \frac{\mu^2 \rho \lambda}{\mu^2 \rho \lambda + (\omega^2 + \lambda^2)(\omega^2 + \mu^2)}, \quad (42)$$

are reduced at all frequencies compared to Eq. 34 and Eq. 37. Therefore we can see that the decay events of X do provide some information about the trajectory $s(t)$, but less than can be obtained from observing the production of X . Since decays of X take place independently of S , from observing the decay of X we can only estimate, based on the lifetime of X , a distribution of times in the past when an S molecule was present. However, observing the production of an X molecule at a given time t tells us directly that at least one S molecule is present. We conclude that in the case where we can observe the entire trajectory of X , decay events provide us with no *additional* information which we could not already extract from the production events contained in the trajectory.

4. Comparison of different motifs

It is important to realise that in motifs I and II considered above the dynamics of the detection reaction affects the statistics of the signal. The gain-to-noise ratios for these motifs are therefore not intrinsic network properties, but also depend on the input process. This can be seen from the appearance of the degradation rate for the input species, λ , in the expressions for the gain-to-noise ratio. In general, therefore, the ensemble of input signals will be different for each motif, making it problematic to directly compare the different information rates. However, we can make a useful comparison in cases in which the input signals have the same form.

First we shall examine motifs II and III, and consider the special case where the statistics of $s(t)$ are the same for both reactions. To achieve this we choose in motif II $\lambda = 0$, and in motif III $\lambda = \rho$. Both motifs can then be described by the same macroscopic evolution equations,

$$\frac{ds}{dt} = \kappa - \rho s(t) + \eta_s(t) \quad (43a)$$

$$\frac{dx}{dt} = \rho s(t) - \mu x(t) + \eta_x(t). \quad (43b)$$

However, the noise correlations will be different in the two cases: for motif II we have $\langle \eta_s(t) \eta_x(t') \rangle = -\rho \langle S \rangle \delta(t - t')$, while for motif III $\langle \eta_s(t) \eta_x(t') \rangle = 0$. Calculating the coherence of these two systems gives

$$\phi^{\text{II}}(\omega) = \frac{1}{4} \quad (44)$$

$$\phi^{\text{III}}(\omega) = \frac{1}{2 + \omega^2/\rho^2}. \quad (45)$$

Since the input power spectra $P_{ss}(\omega)$ are the same for these two networks, we can use the coherence directly as a comparison of signalling performance for signals of different frequencies. We see that at low frequencies, $\omega < \sqrt{2}\rho$, motif III provides more information, while for high frequencies, $\omega > \sqrt{2}\rho$, motif II allows for more reliable signal transmission.

To understand these differing responses of X to signals at different timescales we consider the information that can be extracted from the trace $x(t)$ about S molecules with different lifetimes, as depicted in Fig. 2. The spontaneous decay reaction we have assumed for S means that the lifetimes of different S molecules will be exponentially distributed with mean $1/\rho$. Recall also that the information about the signal $s(t)$ is contained in the timing of the production reactions for X . Since we have taken $\lambda = 0$ in motif II, we know that the decay of every S molecule corresponds to the production of an X . We therefore obtain the same amount of information about the production and decay of each S molecule, regardless of its lifetime. We learn exactly the time at which it decays. In addition we can estimate, based on the typical lifetime of an S molecule, the time at which the molecule was produced. However, for S molecules with a lifetime

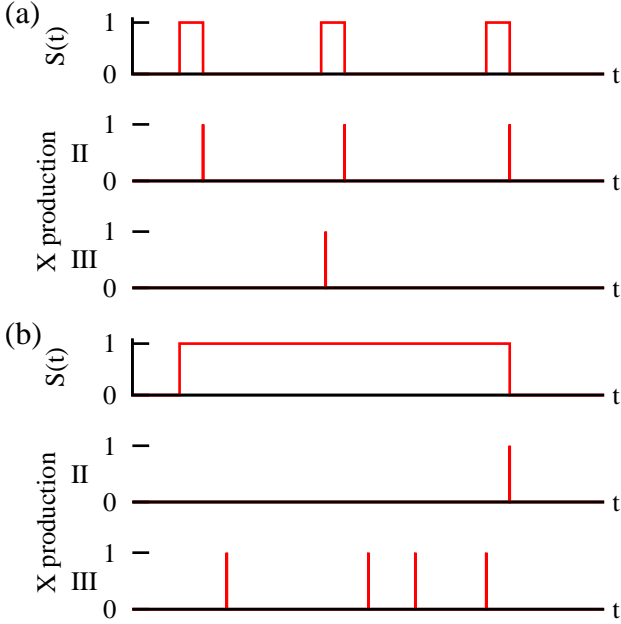


FIG. 2: Comparison of X production in motifs II and III for S molecules with different lifetimes. In each panel the upper plot shows an example of the birth and death of S molecules. The second shows the corresponding timing of X production in motif II. The lower trace shows an example of X production events in motif III. (a) For some short-lived S molecules no X will be produced in motif III. We therefore lose information about these signals, in contrast to motif II for which all S molecules are detected. (b) For long-lived S molecules motif III allows for a more accurate estimate of the production time, since more than one X molecule can be produced. This increases the total information about $s(t)$ compared to motif II.

much longer or shorter than the average this estimate will be inaccurate.

In motif III, on the other hand, X molecules will be produced at an average rate ρ for each S molecule present. Thus for S molecules which decay extremely rapidly with a short lifetime $\tau \ll 1/\rho$, the probability of producing an X molecule will be small. We effectively do not detect these S molecules at all, and hence gain no information about their contribution to the trajectory $s(t)$. This is in marked contrast to motif II, for which we know that we will detect all S molecules. On the other hand, for S molecules with a much longer lifetime $\tau \gg 1/\rho$, more than one X molecule will be produced on average. From this sequence of production events we can estimate both the production and decay times of the corresponding S . Importantly, while we do not get as much information about the decay time as we would in motif II, our estimate of the production time will be more accurate than motif II allows. The total information gained about both the production and decay times may therefore be higher. On average motif III provides more information than motif II about S molecules with a longer than av-

Motif	$g^2(\omega)/N(\omega)$
(I)	$\frac{\alpha\rho}{2\langle Q \rangle} \left[\frac{\lambda}{\omega^2 + \lambda(\lambda + \rho)} \right]$
(Ia)	$\frac{\alpha\rho}{2\langle Q \rangle} \left[\frac{\lambda(\lambda + \rho + \mu)}{(\lambda + \mu)\omega^2 + \lambda(\lambda + \rho)(\lambda + \rho + \mu)} \right]$
(II)	$\frac{\alpha\rho}{2\langle Q \rangle} \left[\frac{\lambda + \rho}{\omega^2 + (\lambda + \rho)^2} \right]$
(III)	$\frac{\alpha\rho}{2\langle Q \rangle} \left[\frac{\lambda}{\omega^2 + \lambda(\lambda + \rho)} \right]$

TABLE II: The gain-to-noise ratio of the reaction motifs in Table I when driven by an upstream signal Q via $Q \xrightarrow{\alpha} Q + S$. The row labelled Ia corresponds to motif I but with the additional reaction $X \xrightarrow{\lambda} \emptyset$.

erage lifetime, but less information about S molecules with a short lifetime. At a more macroscopic level, motif III effectively amplifies slowly-varying signals, producing more than one X molecule for each S , but averages over extremely rapid changes in S , producing less than one X per S . Motif II transmits all signals with a similar amplitude, regardless of the timescale of the input.

Another way to construct a system in which the reactions under comparison do not affect the input signal is to place the input signal upstream of S , and to use this uncorrelated process to drive the reactions of interest. We therefore add to each motif in Table I a signal Q , which drives the production of S via the reaction $Q \xrightarrow{\alpha} Q + S$. This choice ensures that the input signal, now $q(t)$, is uncorrelated from the noise within the downstream signalling network, and hence that the input power spectrum $P_{qq}(\omega)$ is unchanged by the network dynamics. Then the fidelity of signal transmission between $q(t)$ and the output $x(t)$ can be quantified by the gain-to-noise ratio, $g^2(\omega)/N(\omega)$. The gain-to-noise ratios of these modified reaction motifs are shown in Table II.

The expressions in Table II have a number of interesting features. Firstly, we note that for equal reaction rates the gain-to-noise ratios of motifs I and III are identical. In both motifs I and III we can detect the same S molecule many times, either by repeated switching between the S and X forms or because one S can stimulate the production of several X molecules. For these two motifs, with identical rates, one can straightforwardly show that the distribution of the number of times a given molecule converts from S to X and back in motif I is identical to the distribution of the number of X molecules produced from a single S molecule in motif III. Thus the strength of this ‘‘interference’’ between repeated detections of the same S molecule is the same in the two motifs; from the point of view of information transmission, the two reactions are then equivalent.

In the limit $\omega \rightarrow 0$, all three expressions tend to the same value. All three motifs perform equally well for the transmission of slowly-varying signals. For $\omega > 0$ the gain-to-noise ratio for motif II becomes larger than that of either motif I or III, showing that motif II is able to transmit more information. Comparing motifs II and

III, at low frequencies the gain is lower in motif II as we found above when considering signal transmission from S to X . However, the noise is also lower in motif II at all frequencies, because intrinsic noise in the production of S does not propagate to X (see Appendix A for further details). Comparing motifs I and II, the situation is more complex. At low frequencies the gain is smaller in motif II; however, the noise is once again also less in motif II, making these motifs perform equally well for slowly-varying signals. At frequencies $\omega^2 > \mu(\lambda + \rho/2)$ the gain is larger for motif II, as the switching reaction $S \rightleftharpoons X$ is less able to track rapid changes in S . At intermediate frequencies it is possible for motif I to have a lower noise power than motif II. However, in this regime the gain in motif I is significantly smaller than that of motif II, and so motif II is still able to transmit more information at these frequencies.

We can also consider a modified version of motif I in which X molecules can also degrade spontaneously via the same reaction as S , i.e. $X \xrightarrow{\lambda} \emptyset$. We denote this set of reactions by motif Ia, and the corresponding gain-to-noise ratio is shown in Table II. The probability of an X molecule switching back to the S form depends on the relative rates of the two possible decay reactions for X , $X \xrightarrow{\mu} S$ and $X \xrightarrow{\lambda} \emptyset$, and is given by $\mu/(\mu + \lambda)$. In the limit $\mu \rightarrow 0$, this motif reduces to motif II: X molecules never switch back to S but instead always decay. In the limit $\mu \rightarrow \infty$, X molecules always return to the S state, and hence we recover motif I. By varying μ we therefore change the number of times the same molecule switches between the S and X states. We would therefore expect the gain-to-noise ratio for this motif to increase with decreasing μ . We can see from Table II that for any finite non-zero value of μ the gain-to-noise of motif Ia is indeed larger at all frequencies than that of motif I, but not as large as that of motif II. As μ is decreased the gain-to-noise ratio for motif Ia interpolates smoothly between those of motifs I and II, as shown in Fig. 3.

Finally, we examine motifs II and III with the combination of both an upstream signal Q and the parameter choices of Eq. 43: $\lambda = 0$ in motif II and $\lambda = \rho$ in motif III. Specifically, we consider two networks described by

$$\frac{ds}{dt} = \alpha q(t) - \rho s(t) + \eta_s(t) \quad (46a)$$

$$\frac{dx}{dt} = \rho s(t) - \mu x(t) + \eta_x(t), \quad (46b)$$

where as before $\langle \eta_s(t)\eta_x(t') \rangle = -\rho \langle S \rangle \delta(t - t')$ or $\langle \eta_s(t)\eta_x(t') \rangle = 0$ for motifs II and III respectively. For these parameter choices the power spectra of Q and S are the same in both networks.

The gain-to-noise ratios between the input signal $q(t)$

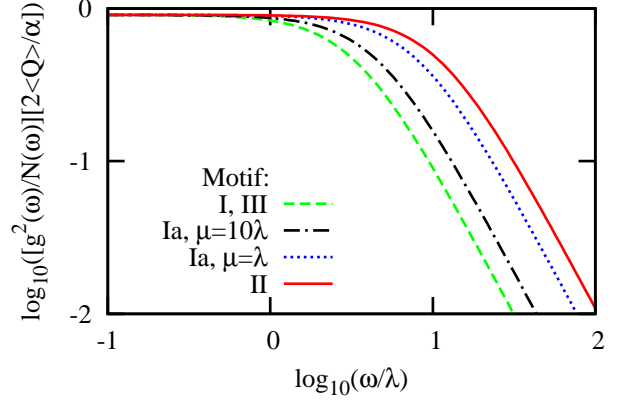


FIG. 3: Gain-to-noise ratio as a function of frequency between $q(t)$ and $x(t)$ for different motifs. The gain-to-noise ratio is highest for motif II, and lowest for motifs I and III. As μ is varied in motif Ia, the gain-to-noise ratio interpolates between these two extremes. In each case $\rho = 10\lambda$ was chosen.

and output $x(t)$ for the two networks are

$$\left[\frac{g^2(\omega)}{N(\omega)} \right]^{\text{II}} = \frac{\alpha}{2\langle Q \rangle} \left[\frac{1}{(\omega/\rho)^2 + 1} \right] \quad (47)$$

$$\left[\frac{g^2(\omega)}{N(\omega)} \right]^{\text{III}} = \frac{\alpha}{2\langle Q \rangle} \left[\frac{1}{(\omega/\rho)^2 + 2} \right]. \quad (48)$$

Interestingly we now find that motif II can transmit low-frequency signals ($\omega \ll \rho$) more reliably than motif III, while for high frequency signals ($\omega \gg \rho$) the two reactions perform equally well. This is in contrast to Eqs 44 and 45, which show that motif III is able to more reliably transmit information about $s(t)$ at low frequencies while motif II is more reliable at high frequencies (see Fig. 4).

To understand how the fidelity of signal transmission changes for different input signals we must consider the different sources and propagation of noise in these networks (see Appendix A for more details). If the input signal is taken to be $s(t)$ then any fluctuations in S , regardless of their origin, contribute to the input signal. However, when we are concerned with the transmission of $q(t)$, fluctuations in $s(t)$ that are uncorrelated from $q(t)$ are considered noise. We wish to transmit only those changes in S that are caused by Q . For the two motifs considered here the mean response to an input signal $q(t)$, measured by the gain between $q(t)$ and $x(t)$, is the same. However, the propagation of intrinsic noise in S differs between the two motifs. We saw previously that motif III is able to amplify fluctuations in S at low frequencies ($\omega \ll \rho$). The fluctuations which made up the signal $s(t)$ in the network described by Eq. 43 now correspond in Eq. 46 to intrinsic noise, independent of $q(t)$, in the production and decay of S . If the input signal of interest is $s(t)$ then amplification of these fluctuations is beneficial, as we saw in Fig. 2, as it allows for better resolution of different $s(t)$ signals. However, if the input signal is

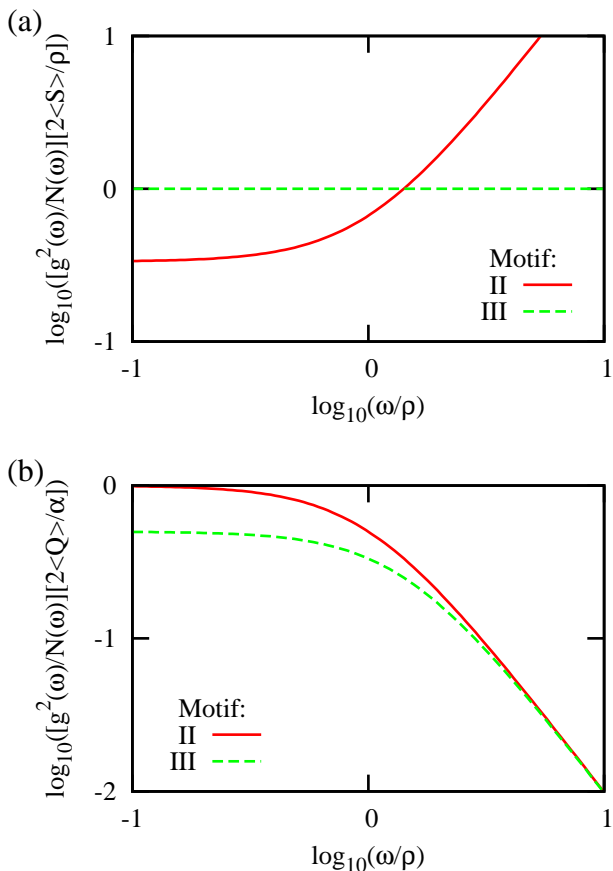


FIG. 4: Comparison of the performance of motifs II and III for the transmission of different input signals. (a) The gain-to-noise for the transmission of $s(t)$ to $x(t)$ for the basic motifs with parameters chosen according to Eq. 43: $\lambda = 0$ in motif II and $\lambda = \rho$ in motif III. (b) Gain-to-noise ratio for the transmission of $q(t)$ to $x(t)$, as in Eq. 46 with the same parameter choice.

$q(t)$, then amplifying intrinsic fluctuations in S , which are uncorrelated from Q , provides no information about $q(t)$; indeed this noise obscures the desired signal. Motif II, meanwhile, does not suffer from this problem as it cannot amplify intrinsic fluctuations in S ; indeed, noise in the production of S is not propagated to X . Consequently at low frequencies the noise in the transmission of $q(t)$ is larger in motif III than in motif II, reducing the fidelity of transmission of these signals. For high frequency ($\omega \gg \rho$) signals we saw previously that motif III is unable to track changes in S , and hence the transmitted noise decreases. The total noise power for motif III is then dominated by intrinsic noise in the production and decay of X , which is the same as that found in motif II. Therefore, the gain-to-noise ratios of the two motifs become the same for high-frequency signals.

IV. DISCUSSION

In this paper we have considered the transmission of time-varying signals through elementary biochemical reactions. We have considered the transmission of both instantaneous signals and of complete trajectories. Our results show that these reactions can have radically different information characteristics for these two types of signals. Most strikingly, for the irreversible modification reaction in motif II the instantaneous information is zero, yet for trajectories we find an extremely large mutual information rate. Additionally for reaction motif III the mutual information rate is independent of the decay rate of the output component, but the instantaneous mutual information does depend on this parameter. These two information quantities therefore measure different aspects of the signalling behaviour of networks, both of which may be important in different biochemical systems.

The reliability with which a network can transmit a particular frequency component of the input signal trajectory is determined by the gain-to-noise ratio of the network as a function of frequency. For systems that obey the spectral addition rule [32], that is those for which downstream reactions do not affect the input signal, the gain-to-noise ratio is an intrinsic property of the processing network. For networks that do not obey the spectral addition rule the gain-to-noise ratio will be dependent on the statistics of the input signal. The mutual information between input and output signals, which quantifies the information which can be transmitted about a particular input ensemble, also depends on the particular choice of the input signal. Thus when comparing the mutual information in different motifs, or the gain-to-noise ratio of motifs for which the statistics of the input signal are affected by the network, care should be taken to ensure that the input distributions of the different networks are the same.

Recently Endres and Wingreen showed [37] that an absorbing detector is able to more accurately measure a steady-state ligand concentration than either a detector that allows for passive observation of the local concentration or a detector to which a ligand can bind reversibly. These different situations are analogous to our motifs II, III and I respectively. It has also been observed previously that the irreversible conversion reaction $S \rightarrow X$ reduces the propagation of noise through networks [32, 38]. Our results in section III B 4 show that the optimal reaction to transmit time-varying signals depends on the input signal that the network is attempting to transmit. If the signal is the concentration of ligand itself, as in Fig. 4(a), then an absorbing detector is beneficial only for rapidly-varying ligand signals, since this reaction does not allow for amplification of slowly-varying signals. To detect low-frequency changes in the ligand signal it is better to respond via a reaction that does not consume the ligand molecule. On the other hand, if the ligand is itself a reporter for another upstream process then the

production reaction of motif III amplifies intrinsic noise in the signalling network at low frequencies, obscuring the signal of interest. In this case, as we saw in Figs. 3 and 4(b), the use of an absorbing detector is always preferable.

The qualitative difference in the relative performance of motifs II and III for different input signals, shown in Fig. 4, has important consequences for the design of signalling cascades. Intuitively we might expect that selecting the reaction for each level of the cascade which provides the most information about the dynamics at the previous level would optimise information transmission for the entire cascade. However, Fig. 4 shows that this is not the case. In fact, choosing the reaction which optimises the reliability of signalling at one downstream step can *reduce* the overall information transmitted through the cascade if more intrinsic noise is propagated. Our results suggest that even in the absence of feedback it is vital to consider the transmission properties of signalling cascades as a whole, rather than isolating individual reaction steps. Naturally-occurring signalling cascades may consist of a number of steps which are individually sub-optimal in terms of one component tracking fluctuations in another, but which together optimise the transmission of the signal of interest while minimising the impact of noise within the network.

We have observed that the information rates for reaction motifs II and III are independent of the decay rate of the output component X . This decay rate sets the relaxation time for intrinsic fluctuations in X and is often considered to set the timescale on which X is able to respond to signals. However, in terms of information transmission this is not the case. Instead of the dissipative timescale, the ability of X to respond to changes in the input signal is determined by the rate of *production* events. Importantly, the mutual information is independent of the decay rate of only the *output* component of a signalling pathway. Information transmission does depend on the relaxation rate of intermediate signalling components. Thus if X is taken as the input to another process then the overall information rate will depend on its relaxation rate, as we saw when considering the decay of X to Y in Section III B 3. More generally, our results indicate that signals in biochemical networks can be encoded in the timing of specific reaction events. To understand whether cells can exploit this information it will be important to investigate situations in which different encoding strategies are employed *in vivo*, and to understand the ability of cells to decode this information.

The mutual information between trajectories, as we have calculated here, is a measure of how reliably signals can be transduced through networks. However, it is known that many biochemical networks also perform other signal-processing functions such as filtering high-

frequency [39] or low-frequency input signals [21, 23]. While these response characteristics of networks appear in the gain-to-noise ratio, as we have shown here and previously [26–28], the mutual information does not distinguish between the properties of the input signal that the cell wishes to respond to and those with which the cell is not concerned. In these cases a more biologically-meaningful measure of the performance of the network would be the mutual information between the properties of interest in the input signal and the output trajectory. For example, if a cell wishes to decode the frequency of an oscillating input signal into the amplitude of a messenger signal, but is not concerned with the amplitude or phase, a more appropriate measure of signalling would be the mutual information between the input signal frequency and the output signal amplitude. The appropriate input and output signals must be considered on a case-by-case basis, and relies on our understanding of the biological function of the particular system being considered. We hope to address these issues in more detail in future work.

Throughout this paper we have calculated information transmission for a Gaussian model of the network of interest. As discussed in Section II, such a model is also able to provide a lower bound on the channel capacity for non-Gaussian systems, provided that the Gaussian model is chosen appropriately. Even for the linear systems considered in Section III, the calculated results are strictly only lower bounds on the channel capacity of real biochemical systems. It is known that for many such systems, particularly for copy numbers of order a few hundred molecules which are often found in signalling networks, the approximation of small Gaussian noise is very accurate [17, 27, 32, 33]. However, in most cases it is not clear what the typical input distributions of biochemical networks in natural environments are. It is therefore difficult to quantify the impact of assuming a Gaussian input distribution in this analysis. We hope that future experiments will clarify the typical distributions of environmental stimuli to which cells are exposed, and which are crucial in determining how information is propagated through networks.

Acknowledgments

We thank Wiet de Ronde for extensive discussions, and Debasish Chaudhuri for a critical reading of the manuscript. This work is part of the research program of the “Stichting voor Fundamenteel Onderzoek der Materie (FOM)”, which is financially supported by the “Nederlandse organisatie voor Wetenschappelijk Onderzoek (NWO)”.

[1] M.B. Elowitz, A.J. Levine, E.D. Siggia, and P.S. Swain. Stochastic Gene Expression in a Single Cell. *Science*,

297:1183–1186, 2002.

- [2] E.M. Ozbudak, M. Thattai, I. Kurtser, A.D. Grossman, and A. van Oudenaarden. Regulation of noise in the expression of a single gene. *Nat. Genet.*, 31:69–73, 2002.
- [3] J.M. Raser and E.K. O’Shea. Control of Stochasticity in Eukaryotic Gene Expression. *Science*, 304:1811–1814, 2004.
- [4] C.E. Shannon. A mathematical theory of communication. *Bell Syst. Tech. J.*, 27:379–423, 623–656, 1948.
- [5] D.M. MacKay and W.S. McCulloch. The Limiting Information Capacity of a Neuronal Link. *Bull. Math. Biophys.*, 14:127–135, 1952.
- [6] F. Attneave. Some Informational Aspects of Visual Perception. *Psychol. Rev.*, 61:183–193, 1954.
- [7] H.B. Barlow. Possible principles underlying the transformations of sensory messages. In W. Rosenblith, editor, *Sensory Communication*, pages 217–234. M.I.T. Press, Cambridge, 1961.
- [8] Laughlin, S.B. A simple coding procedure enhances a neuron’s information capacity. *Z. Naturforsch. C*, 36:910–912, 1981.
- [9] R.R. de Ruyter van Steveninck, G.D. Lewen, S.P. Strong, R. Koberle, and W. Bialek. Reproducibility and Variability in Neural Spike Trains. *Science*, 275:1805–1808, 1997.
- [10] P. Abshire and A.G. Andreou. Capacity and Energy Cost of Information in Biological and Silicon Photoreceptors. *Proc. IEEE*, 89:1052–1064, 2001.
- [11] J. Levine, H.Y. Kueh, and L. Mirny. Intrinsic Fluctuations, Robustness, and Tunability in Signaling Cycles. *Biophys. J.*, 92:4473–4481, 2007.
- [12] G. Tkačik, C.G. Callan, Jr., and W. Bialek. Information flow and optimization in transcriptional regulation. *Proc. Natl Acad. Sci. USA*, 105:12265–12270, 2008.
- [13] G. Tkačik, C.G. Callan Jr., and W. Bialek. Information capacity of genetic regulatory elements. *Phys. Rev. E*, 78:011910, 2008.
- [14] P. Mehta, S. Goyal, T. Long, B.L. Bassler, and N.S. Wingreen. Information processing and signal integration in bacterial quorum sensing. *Mol. Sys. Biol.*, 5:325, 2009.
- [15] G.G. de Polavieja. Reliable biological communication with realistic constraints. *Phys. Rev. E*, 70:061910, 2004.
- [16] T. Tlusty. Rate-distortion scenario for the emergence and evolution of noisy molecular codes. *Phys. Rev. Lett.*, 100:048101, 2008.
- [17] E. Ziv, I. Nemenman, and C.H. Wiggins. Optimal signal processing in small stochastic biochemical networks. *PLoS ONE*, 2:e1077, 2007.
- [18] G. Tkačik, A.M. Walczak, and W. Bialek. Optimizing information flow in small genetic networks. *Phys. Rev. E*, 80:031920, 2009.
- [19] A.M. Walczak, A. Mugler, and C.H. Wiggins. A stochastic spectral analysis of transcriptional regulatory cascades. *Proc. Natl Acad. Sci. USA*, 106:6529–6534, 2009.
- [20] A.M. Walczak, G. Tkačik, and W. Bialek. Optimizing information flow in small genetic networks II: Feed-forward interactions. *Phys. Rev. E*, 81:041905, 2010.
- [21] J.E. Segall, S.M. Block, and H.C. Berg. Temporal comparisons in bacterial chemotaxis. *Proc. Natl Acad. Sci. USA*, 83:8987–8991, 1986.
- [22] S.M. Block, J.E. Segall, and H.C. Berg. Adaptation kinetics in bacterial chemotaxis. *J. Bacteriol.*, 154:312–323, 1983.
- [23] J.T. Mettetal, D. Muzzey, C. Gómez-Uribe, and A. van Oudenaarden. The Frequency Dependence of Osmo-Adaptation in *Saccharomyces cerevisiae*. *Science*, 319:482–484, 2008.
- [24] M.J. Boulware and J.S. Marchant. Timing in Cellular Ca^{2+} Signaling. *Curr. Biol.*, 18:R769–R776, 2008.
- [25] C.J. Marshall. Specificity of Receptor Tyrosine Kinase Signaling: Transient versus Sustained Extracellular Signal-Regulated Kinase Activation. *Cell*, 80:179–185, 1995.
- [26] F. Tostevin and P.R. ten Wolde. Mutual information between input and output trajectories of biochemical networks. *Phys. Rev. Lett.*, 102:218101, 2009.
- [27] W.H. de Ronde, F. Tostevin, and P.R. ten Wolde. The effect of feedback on the fidelity of information transmission of time-varying signals. arXiv:1002.2595.
- [28] W.H. de Ronde, F. Tostevin, and P.R. ten Wolde. *in preparation*.
- [29] P.P. Mitra and J.B. Stark. Nonlinear limits to the information capacity of optical fibre communications. *Nature (London)*, 411:1027–1030, 2001.
- [30] N.G. Van Kampen. *Stochastic Processes in Physics and Chemistry*. North Holland, Amsterdam, 1992.
- [31] P.B. Warren, S. Tănase-Nicola, and P.R. ten Wolde. Exact results for noise power spectra in linear biochemical reaction networks. *J. Chem. Phys.*, 125:144904, 2006.
- [32] S. Tănase-Nicola, P.B. Warren, and P.R. ten Wolde. Signal detection, modularity, and the correlation between extrinsic and intrinsic noise in biochemical networks. *Phys. Rev. Lett.*, 97:068102, 2006; arXiv:q-bio/0508027.
- [33] F.J. Bruggeman, N. Blüthgen, and H.V. Westerhoff. Noise Management by Molecular Networks. *PLoS Comput. Biol.*, 5:e1000506, 2009.
- [34] R.M. Fano. *Transmission of Information: A Statistical Theory of Communications*. MIT Press, Cambridge MA, 1961.
- [35] T.M. Cover and J.A. Thomas. *Elements of Information Theory*. Wiley, New York, 1991.
- [36] T. Munakata and M. Kamiyabu. Stochastic resonance in the FitzHugh-Nagumo model from a dynamic mutual information point of view. *Eur. Phys. J. B*, 53:239–243, 2006.
- [37] R.G. Endres and N.S. Wingreen. Accuracy of direct gradient sensing by single cells. *Proc. Natl Acad. Sci. USA*, 105:15749–15754, 2008.
- [38] E. Levine and T. Hwa. Stochastic fluctuations in metabolic pathways. *Proc. Natl Acad. Sci. USA*, 104:9224–9229, 2007.
- [39] M.R. Bennett, W.L. Pang, N.A. Ostroff, B.L. Baumgartner, S. Nayak, L.S. Tsimring, and J. Hasty. Metabolic gene regulation in a dynamically changing environment. *Nature (London)*, 454:1119–1122, 2008.
- [40] For the purposes of this discussion, a system is considered to be in steady state if it satisfies $\langle S(t) \rangle = \langle S(0) \rangle$ and $\langle S(t)S(t') \rangle = \langle S(t-t')S(0) \rangle$ for all t and t' , and similarly for X .

Appendix A: Comparison of signal and noise partitioning for motifs II and III

Here we consider in more detail the partitioning of the output power $P_{xx}(\omega)$ into signal and noise contributions for transmission from Q to X and from S to X . From the Langevin equations in Eq. 46, where we have chosen $\lambda = 0$ in motif II and $\lambda = \rho$ in motif III, the output power

spectrum of both motifs can be written as

$$P_{xx}(\omega) = \frac{\rho^2}{\omega^2 + \mu^2} \frac{\alpha^2}{\omega^2 + \rho^2} P_{qq}(\omega) + \frac{\rho^2}{\omega^2 + \mu^2} \frac{\Gamma_{ss}}{\omega^2 + \rho^2} + \frac{\Gamma_{xx}}{\omega^2 + \mu^2} + \frac{2\rho^2}{\omega^2 + \mu^2} \frac{\Gamma_{sx}}{\omega^2 + \rho^2}, \quad (\text{A1})$$

where the $\Gamma_{\alpha\beta}$ factors describe the various noise strengths and correlations and are defined by $\langle \eta_\alpha(t)\eta_\beta(t') \rangle = \Gamma_{\alpha\beta}\delta(t-t')$. We note that while we do not specify a particular process or power spectrum for $q(t)$, we have assumed that the noise in S is uncorrelated from Q : $\langle q(t)\eta_s(t') \rangle = 0$ for all t and t' . The first term in Eq. A1 describes the influence of $q(t)$ on $x(t)$ in the absence of noise, and characterises the mean response of $x(t)$ to changes in $q(t)$. The two prefactors to $P_{qq}(\omega)$ represent the effective response functions at the two levels on the cascade, the transmission of Q to S and of S to X . These transfer functions show that high-frequency signals are attenuated at each step. The second term in Eq. A1 includes intrinsic noise in the production and decay of S molecules. The third term similarly describes intrinsic noise in the production and decay of X . For the reactions and parameters we are considering, these three terms are the same for both motifs, with $\Gamma_{ss} = \Gamma_{xx} = 2\alpha\langle Q \rangle$. The final term contains corrections to the two previous noise terms due to correlations between $\eta_s(t)$ and $\eta_x(t)$. For motif III we have $\Gamma_{sx} = 0$. However, for motif II $\Gamma_{sx} = -\alpha\langle Q \rangle$, and this term precisely cancels the intrinsic noise in S . This latter noise, the second term in Eq. A1, contains contributions from the production reactions of S and from the decay reactions. Since this decay occurs via the reaction $S \rightarrow X$ in motif II, these events are also included in the term describing intrinsic noise in the production of X , the third term in Eq. A1. The negative cross-correlation term therefore eliminates the double-counting of these events. Furthermore, the cross-correlation term also removes fluctuations in X due to noise in the production of S . This noise does not propagate to X in motif II, because in the regime of small fluctuations around steady state the spontaneous production and decay of S molecules are two independent Poisson processes; hence noise in the production of S is uncorrelated from the production of X . This is in contrast to motif III, for which production of X molecules can occur whenever an S is present, and hence the signal $x(t)$ depends on the noise in both the production and decay of S . Ultimately, for the two motifs we have

$$P_{xx}^{\text{II}}(\omega) = \frac{\rho^2}{\omega^2 + \mu^2} \frac{\alpha^2}{\omega^2 + \rho^2} P_{qq}(\omega) + \frac{\Gamma_{xx}}{\omega^2 + \mu^2} \quad (\text{A2})$$

$$P_{xx}^{\text{III}}(\omega) = \frac{\rho^2}{\omega^2 + \mu^2} \frac{\alpha^2}{\omega^2 + \rho^2} P_{qq}(\omega) + \frac{\rho^2}{\omega^2 + \mu^2} \frac{\Gamma_{ss}}{\omega^2 + \rho^2} + \frac{\Gamma_{xx}}{\omega^2 + \mu^2}. \quad (\text{A3})$$

If we consider the transmission of Q to X , then only fluctuations in $x(t)$ which are correlated with $q(t)$ should contribute to the signal component of the output power. It also follows from the definition in Eq. 16 that $\Sigma_{q \rightarrow x}(\omega)$ is the same for both motifs,

$$\Sigma_{q \rightarrow x}(\omega) = \frac{\rho^2}{\omega^2 + \mu^2} \frac{\alpha^2}{\omega^2 + \rho^2} P_{qq}(\omega). \quad (\text{A4})$$

The remaining terms in Eq. A1 form the noise power spectrum. For motif II the noise in the output signal is

$$N_{q \rightarrow x}^{\text{II}}(\omega) = \frac{\Gamma_{xx}}{\omega^2 + \mu^2}, \quad (\text{A5})$$

while for motif III we have

$$N_{q \rightarrow x}^{\text{III}}(\omega) = \frac{\rho^2}{\omega^2 + \mu^2} \frac{\Gamma_{ss}}{\omega^2 + \rho^2} + \frac{\Gamma_{xx}}{\omega^2 + \mu^2}. \quad (\text{A6})$$

We can therefore see that the total noise is smaller in motif II than in motif III because, as noted above, noise in the production of S does not propagate to X . However, this difference becomes negligible at high frequencies $\omega \gg \rho$ because at these frequencies motif III effectively averages over rapid fluctuations in S and hence the effect of these fluctuations on X diminishes.

Now suppose that we take $s(t)$, rather than $q(t)$, to be the input signal to the network. Then the signal component of the output power should include those terms for which X is correlated with S . For motif III we can straightforwardly see that the second term in Eq. A1, which describes fluctuations in $x(t)$ due to intrinsic noise in S , should contribute to the signal power. The intrinsic fluctuations in X remain uncorrelated from S , and hence are still considered noise. We therefore have

$$\Sigma_{s \rightarrow x}^{\text{III}}(\omega) = \frac{\rho^2}{\omega^2 + \mu^2} \left[\frac{\alpha^2}{\omega^2 + \rho^2} P_{qq}(\omega) + \frac{\Gamma_{ss}}{\omega^2 + \rho^2} \right] \quad (\text{A7})$$

$$N_{s \rightarrow x}^{\text{III}}(\omega) = \frac{\Gamma_{xx}}{\omega^2 + \mu^2}. \quad (\text{A8})$$

We can also identify the bracketed terms in Eq. A7 as the power spectrum of S . If we consider motif II, while $P_{xx}(\omega)$ does not depend on $\eta_s(t)$ explicitly we must recall that noise in the production of X molecules corresponds to noise in the decay of S , and hence contributes to the signal power. Applying the definition of the signal power, Eq. 16, leads to the following result:

$$\Sigma_{s \rightarrow x}^{\text{II}}(\omega) = \frac{\rho^2}{\omega^2 + \mu^2} \frac{\alpha^2}{\omega^2 + \rho^2} P_{qq}(\omega) + \frac{\Gamma_{sx}}{\omega^2 + \mu^2} \frac{\Gamma_{sx}}{[\alpha^2 P_{qq}(\omega) + \Gamma_{ss}]} \quad (\text{A9})$$

$$N_{s \rightarrow x}^{\text{II}}(\omega) = \frac{\Gamma_{xx}}{\omega^2 + \mu^2} - \frac{\Gamma_{sx}}{\omega^2 + \mu^2} \frac{\Gamma_{sx}}{[\alpha^2 P_{qq}(\omega) + \Gamma_{ss}]} \quad (\text{A10})$$

The noise in motif II is again lower than in motif III at all frequencies. In this case, this difference arises because

in motif II noise in the production of X is correlated with $s(t)$. To study the differences between the signal powers of the two motifs we consider

$$\begin{aligned} \Delta\Sigma(\omega) &= \Sigma_{s \rightarrow x}^{\text{II}}(\omega) - \Sigma_{s \rightarrow x}^{\text{III}}(\omega) \\ &= \frac{\Gamma_{ss}}{\omega^2 + \mu^2} \left[\frac{\Gamma_{ss}}{4(\alpha^2 P_{qq}(\omega) + \Gamma_{ss})} - \frac{\rho^2}{\omega^2 + \rho^2} \right], \quad (\text{A11}) \end{aligned}$$

where we have used the facts that Γ_{ss} is the same for both motifs and that for motif II $\Gamma_{sx} = -\Gamma_{ss}/2$. We can see that at low frequencies $\omega \ll \rho$, $\Delta\Sigma(\omega)$ is negative,

showing that the signal power is larger in motif III than in motif II. This reflects amplification of low-frequency noise in $s(t)$ by motif III. At high frequencies motif III is no longer able to amplify noise, and instead at the level of X averages over these fluctuations. In this regime $\Delta\Sigma(\omega)$ becomes positive, showing that the signal power is larger in motif II than in motif III. This transition results in the cross-over observed in Fig. 4(a) between the different frequency regimes in which motif II or III can more reliably transmit signals.